Appl. Phys. B 63, 145–150 (1996)

Applied Physics B Lasers and Optics

Parallel guiding of signal beams by a ring dark soliton

A. Dreischuh*, V. Kamenov*, S. Dinev

Sofia University, Department of Physics, 5, J. Bourchier Blvd., BG-1164 Sofia, Bulgaria
(Fax: + 43-316/873-8655; E-mail: SASCHA@fexphal101.tu-graz.ac. at)

Received: 8 September 1995/Accepted: 13 February 1996

Abstract. Guiding of multiple signal beams in an induced all-optical cable is studied theoretically. A balance relation is derived for the interaction geometry and undistorted propagation of bright elliptical signal beams nested in a single ring dark soliton. The numerical analyses show a remarkable misalignment stability of the parallel guiding scheme.

PACS: 42.65

The Dark Spatial Solitons (DSS) are self-supported intensity-dips imposed on background beams of high intensities [1, 2]. The physical mechanism of their formation is based on the balanced counteraction of beam diffraction and self-defocusing. Both 1D and 2D DSS require a negative nonlinear correction $n_2|E|^2 < 0$ to the medium refractive index

$$n = n_0 + n_2|E|^2, \tag{1}$$

where E is the electric field amplitude of the background beam. The refractive index near the DSS center remains higher as compared to the refractive index in it's wings. Therefore, the DSS should obey spatial guiding properties, similar to these of bright spatial solitons at $n_2 > 0$ [3]. It is shown, that a short dark solitary wave can propagate undistorted in the otherwise forbidden anomalous dispersion regime when it is coupled to a bright pulse in the anomalous dispersion regime [4] in the form of a symbiotic pair [5]. Bright optical pulses could be simultaneously guided and compressed by dark solitons [6]. It was demonstrated recently, that a quasi-steady-state photorefractive spatial soliton can form a waveguide structure able to guide powerful beams at longer wavelengths [7]. The guiding feature of DSS has been proved by the experimental investigation of optical vortex solitons [8, 9]. Recently, the existence of 2D Ring Dark Solitons (RDS) has been predicted [10, 11]. 2D RDSs are already generated at a pure amplitude modulation of the background beam at the entrance of the nonlinear medium [12, 13]. The analyses showed [11, 14] that the transverse velocity of the RDS along the nonlinear propagation path can be minimized by suitably chosen odd initial conditions (i.e. at diametrical π phase jumps centered at the zero-intensity points of the "black" ring).

In this paper we present a theoretical study of an induced all-optical communication cable. The ring dark soliton guiding cable can be induced, in principle, instantly in any direction in a volumetric media, guiding multiple signal beams, which makes it attractive for the extreme high-capacity short-distance communications. A simple analytical relationship on the geometry of the guiding scheme is derived and balance conditions, including spatial profile, ellipticity and initial peak intensity are found for undistorted multiple bright beam propagation. A remarkable stability against misalignment of the signal beam with respect to the RDS is found.

1 Variational analysis

The physical mechanism underlying the guiding of a probe beam by a RDS (Fig. 1a) is the Induced Phase Modulation (IPM) [15] on the signal beam. In view of the weaker expressed transverse dynamics of the RDS at larger ring radii [10, 11, 14], such a dark ring could be approximated by an 1D odd DSS [1, 2] if the ring radius is much higher than the ring width (Fig. 1b). Both dark formation and bright signal beam plotted on Fig. 1 are grayscale-coded. We will show that the 1D odd DSS forms a gradient planar waveguide of nonlinear cladding. Under suitably chosen balance conditions an elliptical beam can propagate undistorted along this waveguide. The higher diffraction along the short axis x of the ellipce could be compensated by the combined action of the IPM (at $n_2^{IPM} < 0$) and the weaker Self-Phase Modulation (SPM) of the bright signal (at $n_2^{SPM} > 0$). The only SPM

*Present address: Technical University Graz, Institute of Experimental Physics, Petersgasse 16, A-8010 Graz, Austria

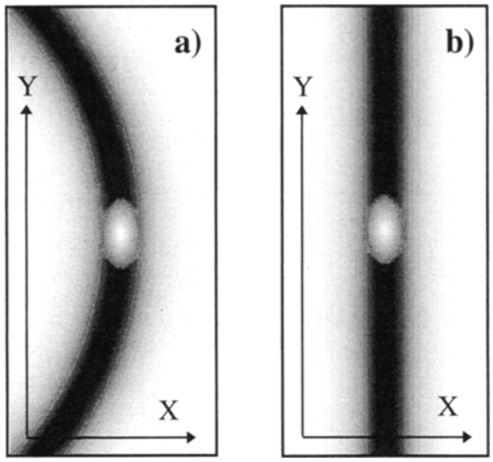

Fig. 1a, b. Simplified scheme analyzed: Ring dark soliton with a large radius (**a**) forming a curved waveguide is approximated by a dark soliton stripe (**b**) equivalent to a planar waveguide with a nonlinear cladding. The position of the elliptical signal beam is indicated too

preserves for the elliptical signal beam diffraction spreading along the linearly diffraction nonlimited coordinate y. This situation could be realized, for example, if the doubled frequency of the pump is on the blue side of a two-photon resonance, the doubled signal-frequency-on the red side, whereas the sum of these frequencies is even less blue-shifted from the two-photon transition [16, 17]. The strengths of the SPM and IPM could be varied independently by changing the pump- and signal detunings. Another possible way to ensure these conditions is to use a nonlinear medium, in which the nonlinearities for the RDS self-action and IPM (e.g. photorefractive [7]) are of a different origin as compared to this for the signal SPM (e.g. electronic).

The 2D nonlinear evolution of signal beam along the nonlinear medium is described [10, 11] by

$$i\frac{\partial \Psi_s}{\partial z} + \alpha\left(\frac{\partial^2}{\partial x^2} + \frac{\partial^2}{\partial y^2}\right)\Psi_s + k^{SPM}|\Psi_s|^2\Psi_s + k^{IPM}|\Psi_p|^2\Psi_s = 0\,, \tag{2}$$

where Ψ_s and Ψ_p are the complex slowly-varying amplitudes of the bright signal beam and of the pump (1D dark soliton stripe) respectively, $\alpha = (1/2k_s)$, k_s is the wave-number of the signal wave, $k^{SPM}(\lambda_s) = n_2^{SPM}(\lambda_s)k_s/(2n_{0s})$ and $k^{IPM}(\lambda_s) = n_2^{IPM}(\lambda_s;\lambda_p)k_s/(2n_{0s})$ accounting for the SPM and IPM respectively.

We analyzed (2) by using the variational approach [18, 19]. Equation 2 could be considered as an Euler-Lagrange equation for the Lagrangian

$$L = (i/2)\left[\Psi_s\frac{\partial \Psi_s^*}{\partial z} - \Psi_s^*\frac{\partial \Psi_s}{\partial z}\right] + \alpha\left[\left|\frac{\partial \Psi_s}{\partial x}\right|^2 + \left|\frac{\partial \Psi_s}{\partial y}\right|^2\right] - k^{SPM}(\lambda_s)|\Psi_s|^4/2 - k^{IPM}(\lambda_s;\lambda_p)|\Psi_s|^2|\Psi_p|^2. \tag{3}$$

In order to avoid the necessity to modify the Lagrangian according to the asymptotically nonwanishing background of the RDS [20] we "inverted" the physical picture on the following way. The phase distribution induced by the dark soliton stripe (see Fig. 1b) on the signal at $n_2^{SPM}(\lambda_p) < 0$ should be the same as the phase distribution induced by a "bright" soliton stripe at $n_2^{SPM}(\lambda_p) > 0$ [21]. Therefore, one can consider an elliptical Gaussian signal beam of the form

$$\Psi_s(x,y,z) = \frac{A_s(z)}{\omega_{sx}(z)\omega_{sy}(z)}\exp\left[-\frac{x^2}{a_{sx}^2\omega_{sx}^2(z)} - \frac{y^2}{a_{sy}^2\omega_{sy}^2(z)}\right] \times \exp\left[-\frac{ik_s}{2}(\rho_{sx}(z)x^2 + \rho_{sy}(z)y^2)\right] \tag{4a}$$

guided by a quasi-2D (inverted) Gaussian pump beam:

$$\Psi_p(x,y,z) = \frac{A_p(z)}{\omega_{px}(z)}\exp\left[-\frac{x^2}{a_{px}^2\omega_{px}^2(z)}\right]\exp\left[-\frac{ik_p\rho_{px}(z)x^2}{2}\right]. \tag{4b}$$

It should be kept in mind, that the formation of a DSSs at $n_2^{SPM}(\lambda_p) > 0$ is unphysical. In (4a, b) A_s and A_p are the slowly-varying amplitudes of the signal and ("inverted") pump, respectively, ω_{ix} and ω_{iy}, (i = s,p) are the normalized radii of the beams $[\omega_{ix,y}(z=0) = 1]$, $a_{ix,y}$ are their initial physical radii at $1/e$-level, and $\rho_{ix,y}$ are functions of the inverse radii of curvature of the respective wavefronts $[\rho_{ix,y}(z=0) = 0$ in a plane-wave approximation]. Note, that the formal "inversion" of the 1D DSS (Fig. 1b) requires a modification of it's phase distribution to a plane one. In the opposite case splitting of the "inverted" pump should be expected [2].

Following the variational procedure [18, 19] at $\omega_{px}(z) = 1$ and $\rho_{px}(z) = 1$ we obtained the following system of ordinary differential equations for the normalized signal beam radii:

$$\frac{d^2\omega_{sx}}{dz^2} = \frac{4}{k_s^2 a_{sx}^4\omega_{sx}^3} - \frac{k^{SPM}(\lambda_s)|A_s|^2}{k_s a_{sx}^2\omega_{sx}^3\omega_{sy}} - \frac{4\omega_{sx}k^{IPM}(\lambda_s;\lambda_p)|A_p|^2 a_{px}}{k_s(a_{px}^2 + a_{sx}^2\omega_{sx}^2)^{3/2}} \tag{5a}$$

$$\frac{d^2\omega_{sy}}{dz^2} = \frac{4}{k_s^2 a_{sy}^4\omega_{sy}^3} - \frac{k^{SPM}(\lambda_s)|A_s|^2}{k_s a_{sy}^2\omega_{sy}^3\omega_{sx}^2}. \tag{5b}$$

From the requirement for a diffraction-compensated propagation of the signal along the y-axis $(\partial^2\omega_{sy}/\partial z^2 = 0)$ we obtain the square of the signal field-amplitude required

$$|A_s|^2 = \frac{4\omega_{sx}^2}{k_s a_{sy}^2 k^{SPM}(\lambda_s)}. \tag{6a}$$

The analogous requirement along the x-axis yields, that

$$k^{IPM}|A_p|^2 a_{px} = \frac{(a_{px}^2 + a_{sx}^2)^{3/2}}{k_s a_{sx}^2}\left(\frac{1}{a_{sx}^2} + \frac{1}{a_{sy}^2}\right). \tag{6b}$$

Diffractionless propagation of the pump along the x-axis can be expected if the diffraction and nonlinear lengths ($L_{Diff}^p = k_p a_{px}^2$ and $L_{NL}^p = 1/(k^{SPM}(\lambda_p)|A_p|^2)$, respectively) are equal. Therefore, (6b) takes the form

$$[1 - (a_{sx}/a_{sy})^2]^2 = \frac{4}{(a_{px}/a_{sx})^2[(a_{px}/a_{sx})^2 + 1]^3}. \tag{6c}$$

For simplicity, in deriving (6c) $k^{SPM}(\lambda_p) = k^{SPM}(\lambda_s) = k^{IPM}(\lambda_s; \lambda_p)/2$ is assumed. This equation allows to estimate approximately the initial relative dimensions a_{sx}/a_{sy} and a_{px}/a_{sx} of the pump and signal beam corresponding to a diffractionless propagation of an elliptical beam under SPM and IPM.

2 Numerical results

The simple relationship given by (6c) is derived under two important assumptions, which validity will be verified in the following:
i) The RDS is approximated by an 1D dark soliton stripe;
ii) The dark stripe at $n_2^{SPM}(\lambda_p) < 0$ is analyzed as a "bright" one-dimensional spatial "Gaussian" soliton at $n_2^{SPM}(\lambda_p) > 0$.

The dynamics of the RDS is modelled on the base of the normalized Schrödinger equation

$$i\frac{\partial \Psi_p}{\partial z} + \frac{1}{2L_{Diff}}\left(\frac{\partial^2}{\partial \xi^2} + \frac{\partial^2}{\partial \eta^2}\right)\Psi_p + \frac{1}{L_{NL}}(C|\Psi_p|^2 + 2|\Psi_s|^2)\Psi_p = 0\,. \tag{7a}$$

The evolution of the bright elliptical signal beam (at $n_2^{SPM}(\lambda_s) > 0$) located in a 2D RDS (at $n_2^{SPM}(\lambda_p) = -n_2^{SPM}(\lambda_s)$ and $n_2^{IPM}(\lambda_s; \lambda_p) = 2n_2^{SPM}(\lambda_p)$) is studied by solving the (2 + 1)D nonlinear Schrödinger equation [see (2)]

$$i\frac{\partial \Psi_s}{\partial z} + \frac{1}{2L_{Diff}}\left(\frac{\partial^2}{\partial \xi^2} + \frac{\partial^2}{\partial \eta^2}\right)\Psi_s + \frac{1}{L_{NL}}(|\Psi_s|^2 - 2C|\Psi_p|^2)\Psi_s = 0\,, \tag{7b}$$

where the dimensionless transverse spatial coordinates ξ and η are normalized to the shorter ellipce axis a_{sx}, L_{NL} is the signal nonlinear length, L_{Diff}-the signal diffraction length along a_{sx}, and $C = |A_p|^2/|A_s|^2$. According to (6c) we choose $a_{sx} = a_{px} = 1$, $a_{sy} = 1.85$, $|A_p|^2 = 1$ and $|A_s|^2 = 0.3$. If desired, the normalized propagation distance z/L_{Diff} could be expressed in units of signal-beam diffraction lengths with respect to the larger ellipce-axis by multiplying it by a factor of $(a_{sx}/a_{sy})^2$. Dark odd ring of an initial radius $R_0 = 28.5$ times the ring width a_{px} is assumed in this work.

Figure 2 plots a radial cross-section (Fig. 1a) of the RDS (dotted curve) and the signal beam (solid curve) nested within the ring. The 2D RDS is described by

$$\Psi_p = A_p B(r)\tanh[(r - R_0)/r_0]\exp(i\Phi),\ r_0 = a_{px}\,, \tag{8a}$$

where

$$B(r) = \exp\{-(r/40)^{10}\} \tag{8b}$$

is the super-Gaussian background beam. The signal is assumed to have an initial profile, given by

$$\Psi_s = A_s\,\mathrm{sech}[(x - x_0)/a_{sx}]\,\mathrm{sech}[(y - y_0)/a_{sy}]\,. \tag{8c}$$

The corresponding coordinates of the signal beam center are (x_0, y_0), $(x_0^2 + y_0^2 = R_0^2$ at a perfect alignment of the signal with respect to its' radial width), $\Phi(r)$ represents the phase portrait of the RDS [10, 11, 13].

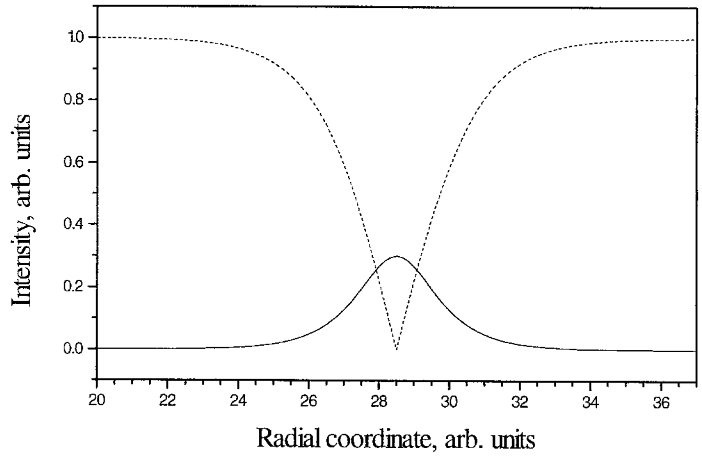

Fig. 2. Initial radial intensity distribution of a RDS (*dotted curve*) and of an elliptical signal beam (*solid curve*) used for the simulations ($a_{sx} = a_{px} = 1$, $a_{sy} = 1.85$, $|A_p|^2 = 1$ and $|A_s|^2 = 0.3$)

The numerical procedure used is a 2D generalization of the beam-propagation method. Both dark and bright formation are discretisized over 1024×1024 grid points.

At this point it should be noted, that at least three approaches to reduce the dynamics of the RDS does exist. First, the whole background could be suitably focussed. This focussing allows to extend gradually the distance, at which the RDS will become broader as initially [10]. Second, the RDS-divergence could be reduced by using a smoother dark ring of a larger radius R_0 [14]. Third, the background within the ring only could be initially phase modulated as done by a focusing lens of an aperture R_0. In this case the RDS decreases initially its radius and thereafter starts diverging with nearly the same transverse velocity as the unmodulated RDS. For example, if the radius of curvature of the phasefront within the ring is chosen to be twice the RDS radius R_0, the propagation distance, at which R_0 becomes 0.4% higher its initial value is twice longer as compared to that in the unperturbed case. Although the latter results will be discussed in greater details elsewhere, further we will compare the signal evolution within a "frozen" and "dynamical" RDS by solving (7b), respectively (7a, b).

The lower solid curve in Fig. 3 plots the evolution of the signal-beam peak intensity along the nonlinear medium up to a distance $z/L_{Diff} = 35$. In this calculation the RDS is treated as a static formation. As seen, the signal beam peak intensity oscillates periodically and decreases approaching an asymptotical value of 0.86 of it's initial value. This behavior could be attributed to both the tanh-radial profile of the RDS and the sech-profile of the signal beam assumed, as well as to the finite value of the RDS radius R_0 ($R_0 \to \infty$ refers to the 1D dark soliton stripe considered variationally). Therefore, the approximate initial values of $a_{sx,y}$ and $a_{px} = r_0$ given by (6c) could be evaluated as reasonable ones. The lower dashed curve in Fig. 3 represents the evolution of the signal peak intensity influenced by the divergence and the contrast-reduction of the RDS when its inherent dynamics is not to be

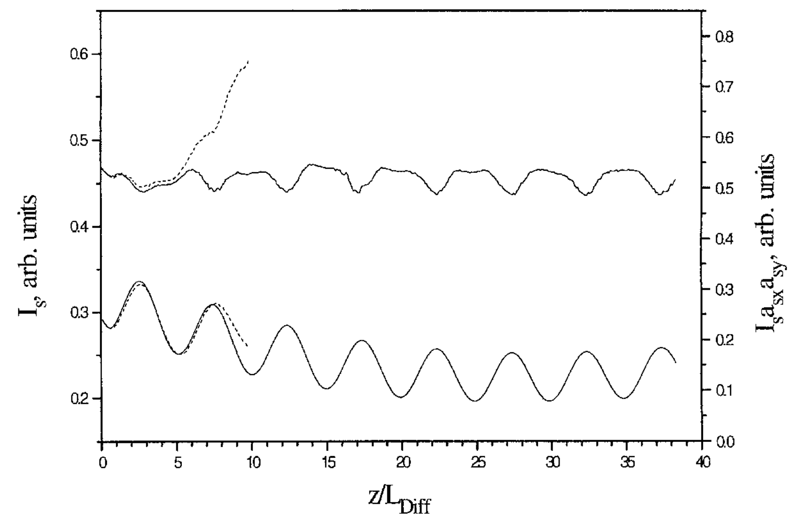

Fig. 3. Evolution of the guided signal-beam peak-intensity I_s (*lower two curves*) and of the quantity $I_s a_{sx} a_{sy}$ (*upper curves*) along the nonlinear medium. The *solid lines* refer to the static RDS, the *dashed* ones-to a diverging RDS

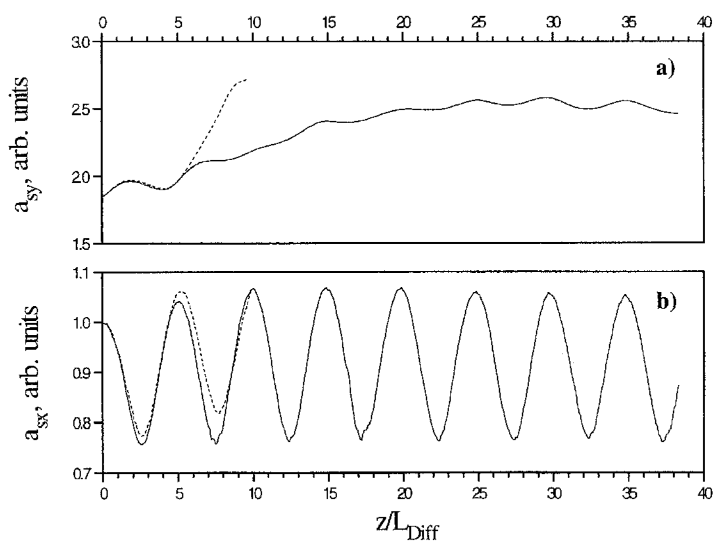

Fig. 4a, b. Evolution of the signal beam width along the longer (**a**) and the shorter (**b**) axis of the ellipce. The *solid lines* refer to the static RDS, the *dashed* ones-to a diverging RDS

neglected. After a propagation distance of about $7.5L_{Diff}$ the signal intensity reduces significantly.

For circularly-symmetrical self-supported formations the intensity multiplied by the second power of the beam/pulse width is a constant. Although the signal-beams analyzed are elliptical ones, the upper two curves in Fig. 3 plot $I_s a_{sx} a_{sy}$ vs. z/L_{Diff} in the case of a nondiverging (solid curve) and diverging RDS (dashed). If the dynamics of the guiding RDS is negligible, the quantity $I_s a_{sx} a_{sy}$ seems to conserve asymptotically as a result of the stabilization of the large-ellipce radius a_{sy} (Fig. 4a, solid curve). The periodic oscillations are due to the oscillations in the short-ellipce radius a_{sx} (Fig. 4b, solid curve) in the RDS. The low-depth short-distance oscillations in $I_s a_{sx} a_{sy}$ (Fig 3, upper solid curve) are caused by the finite numerical discretization resulting in a 0.4% inaccuracy in determining the beam widths. For comparison, the upper dashed curve in Fig. 3 plots the quantity $I_s a_{sx} a_{sy}$ for the signal being guided by a "dynamic" RDS. Its significant increase should be attributed mainly to the increment of the signal-beam radius a_{sy} along the ring-arc, since a_{sx} increases relatively slower (Fig. 4b, dashed curve). It should be mentioned, that the signal beam evolution up to $7.5L_{Diff}$ does not seems to be strongly influenced by the RDS dynamics. If larger distances of guiding are desired, the initial conditions in the generation of the RDS should be suitably manipulated.

Figure 5 presents grayscale plots of the static RDS and the elliptical signal beam nested in at the entrance of the nonlinear medium (a) and after 36 diffraction lengths. For comparison, Fig. 5c presents the RDS and the signal beam at $z = 10L_{Diff}$ at a negligible signal SPM. The signal becomes wider in radial direction, but continues to be guided by the RDS. Along the RDS-arc, however, the signal spreads significantly due to the diffraction.

Let us assume, that multiple bright elliptical signal beams are to be guided by a single RDS (Fig. 6). From practical point of view the requirement for a negligible cross-talk between the information channels is an obligatory one. This mode of propagation can be realized at suitably chosen signal-beam ellipticity and signal peak-intensity. The spatial SPM should compensate for the

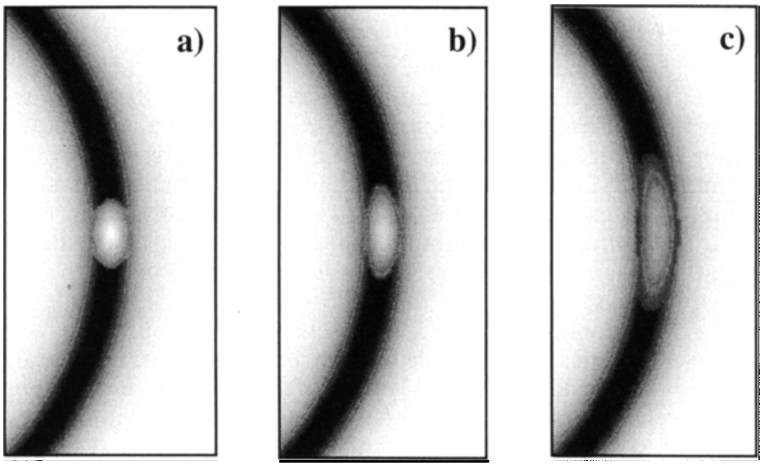

Fig. 5a–c. Grayscale images of the RDS and the bright signal nested in at the entrance of the nonlinear medium (**a**) and at $z = 36L_{Diff}$ (**b**). For comparison the signal beam intensity distribution at $z = 10L_{Diff}$ resulting from a negligible SPM is shown on (**c**)

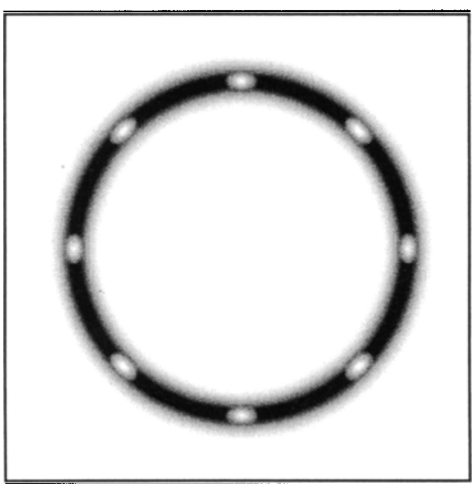

Fig. 6. Grayscale plot of 8 elliptical signal beams being guided simultaneously by a single static RDS up to $z = 36L_{Diff}$. The parameters of the simulation are the same as for Fig. 2.

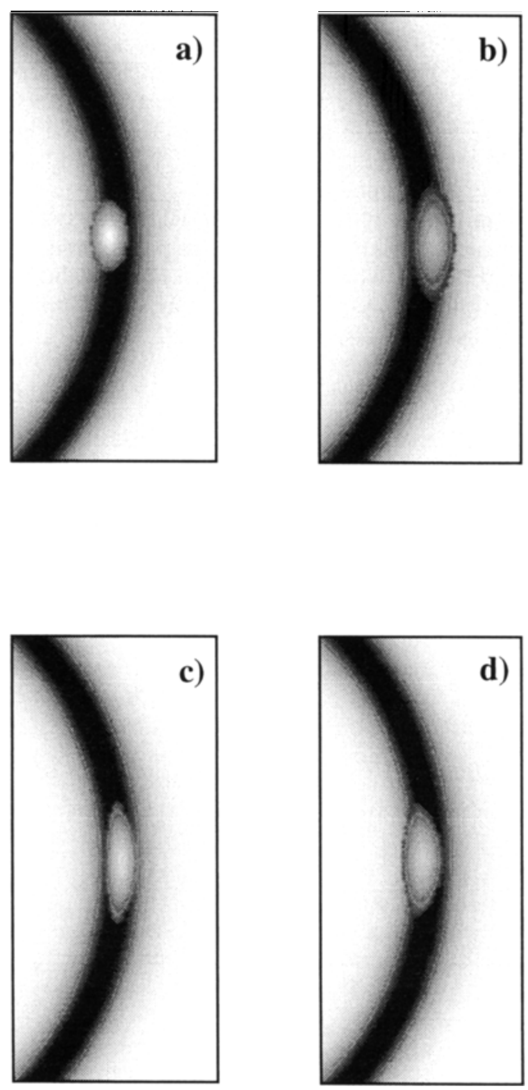

Fig. 7a–d. Misalignment stability of the guiding scheme: Initially deviated signal beam (**a**: offset-90% of the ring width) remains well allocated in (**b**: $z = 30L_{Diff}$; **c**: $z = 32.5L_{Diff}$; **d**: $z = 35L_{Diff}$)

azimuthal diffraction spreading. At a certain RDS radius R_0 the higher number of signal beams to be guided parallely (without a cross-talk) should require reduced ellipticities and, therefore, higher intensities of the signals. The numerical result in Fig. 6 refers to a simultaneous guiding (up to $z = 36L_{Diff}$) of eight signal beams of sech-profiles and of ellipticities equal to 1.85 by a static RDS. Their initial peak-intensities are 30% of the background intensity required for the dark soliton formation (see also Fig. 2). As could be seen on Fig. 6, there is no cross-talk between the signal beams.

An important parameter of this parallel guiding-scheme is the guiding stability against initial nonperfect alignments of the signal beams with respect to the RDS irradiance minimum. Figure 7 illustrates a remarkable stability of the guiding-scheme considered. The signal beam deviated initially at $0.9r_0$ with respect to the RDS intensity-dip (Fig. 7a) remains well allocated in the dark ring at $z = 30L_{Diff}$ (Fig. 7b) and continues to oscillate around the ring minimum (Fig. 7d, $z = 35L_{Diff}$) passing radially through (Fig. 7c, $z = 32.5L_{Diff}$). These results refer to the case of a negligible RDS transverse dynamics. In general, the nonzero transverse velocity of the RDS could influence negatively the signal guiding-stability. Figure 8 shows, however, that the offset of the signal beam (dashed curve) with respect to the RDS intensity-minimum (solid curve) does not exceed 20% the soliton radius at $z/L_{Diff} = 4.5$ and decreases monotonically up to $z/L_{Diff} = 10$ even at significant changes of the signal-beam dimensions (Fig. 4a, b, dashed curves). Nevertheless, a suitable manipulation of the initial conditions in the generation of the guiding RDS would allow to preserve, at least partially, for the signal-beam spatial-profile changes.

In view of the above, we believe, that a parallel guiding of multiple signal beams by a RDS could be observed experimentally. For this purpose it is necessary to select a nonlinear medium, for which both $n_2^{SPM}(\lambda_p)$ and $n_2^{IPM}(\lambda_s; \lambda_p)$ are negative, whereas $n_2^{SPM}(\lambda_s)$ is positive. This requirement could be fulfilled in "proof-of-principle" experiments in resonant nonlinear media [22], but it's practical applicability should be verified on the base of suitable semiconductor-doped glasses, glass-composites [23, 24] or photorefractive media [7]. For communication purposes signal pulses should be considered instead of beams. The influence of the medium group-velocity dispersion, IPM and SPM on the signal pulse shape [25] should be a subject of a separate detailed analysis.

Further data on the reduction of the RDS transverse velocity by an appropriate change of the parameters of RDS and signal beams, which would open the possibility for a multifunctional short-range high-capacity communication will be discussed elsewhere.

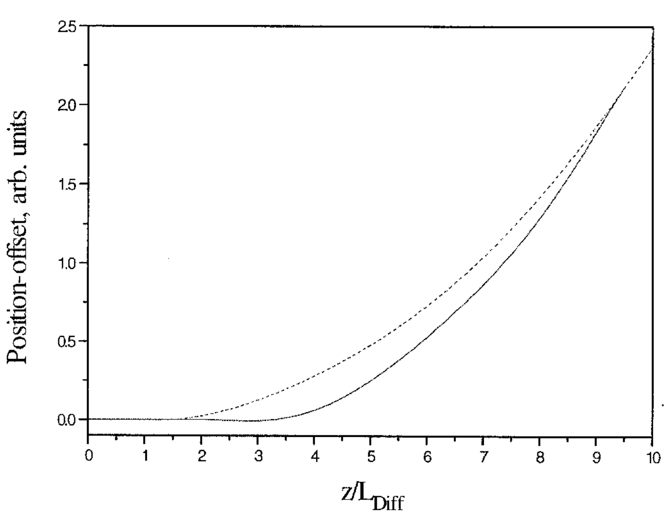

Fig. 8. Offset of the ring and the signal beam (*solid* and *dashed curves*, respectively) from their initial positions on the background vs. normalized propagation distance as a result of the RDS divergence

Conclusion

We believe, we have proposed a practical scheme for parallel guiding of multiple signal beams by RDSs. Cross-talk-free signal guiding can be achieved as a result of the compensation of the signal diffraction spreading by the SPM and IPM. The initial signal-beam ellipticity required seems easily obtainable by using semiconductor laser sources. The guiding stability with respect to the signal beam radial misalignments from the RDS intensity-minimum is found to be relatively high. A future spatio-temporal analysis of this scheme could open the way practically applicable optical communication-cable to be constructed. In view of the different scenarious of the instability dynamics of the quasy-one-dimensional dark solitons [26], special attention should be paid to the modulational stability of the guiding RDS.

Acknowledgements. The authors are indebted to the Technical University Graz, Austria, for the warm hospitality and for the CPU time during the final stages of this work. This work was supported by the National Science Fund, Bulgaria by a grant F-424.

References

1. D. Anderson, D. Hooton, G. Swartzlander, Jr., A. Kaplan: Opt. Lett. **15**, 783 (1990)
2. G. Swartzlander, Jr., D. Anderson, J. Regan, H. Yin, A. Kaplan: Phys. Rev. Lett. **66**, 1583 (1991)
3. J.U. Kang, G.I. Stegeman, J.S. Aitchison: Opt. Lett. **20**, 2069 (1995)
4. S. Trillo, S. Wabnitz, E. Wright, G. Stegeman: Opt. Lett. **13**, 871 (1988)
5. M. Lisak, A. Höök, D. Anderson: J. Opt. Soc. Am. B **7**, 810 (1990)
6. R. Jin, M. Liang, G. Khitrova, H.M. Gibbs, N. Peyghambarian: Opt. Lett. **18**, 494 (1993)
7. M. Morin, G. Duree, G. Salamo, M. Segev: Opt. Lett. **20**, 2066 (1995)
8. G. Swartzlander, Jr., C. Law: Phys. Rev. Lett. **69**, 2506 (1992)
9. C. Law, G. Swartzlander, Jr.: Opt. Lett. **18**, 586 (1993)
10. Yu. S. Kivshar, X. Yang: Phys. Rev. E **50**, R40 (1994)
11. Yu. S. Kivshar, X. Yang: Chaos, Solitons & Fractals **4**, 1745 (1994)
12. S. Baluschev, A. Dreischuh, I. Velchev, S. Dinev, O. Marazov: Appl. Phys. B **61**, 121 (1995)
13. A. Dreischuh, W. Fließer, Velchev, S. Dinev, L. Windholz: Appl. Phys. B **62**, 139 (1996)
14. V. Kamenov, A. Dreischuh, S. Dinev: Physica Scripta (submitted)
15. R. De la Fuente, A. Barthelemy: IEEE J. QE-**28**, 547 (1992)
16. R. Saxena, I. McMichael, P. Yeh: Appl. Phys. B **51**, 243 (1990)
17. S. Dinev, A. Dreischuh, D. Kavaldjiev, K. Krastev: J. Opt. Soc. Am. B **9**, 387 (1992)
18. D. Anderson: Phys. Rev. A **27**, 3135 (1983)
19. M. Karlsson, D. Anderson, M. Desaix: Opt. Lett. **17**, 22 (1992)
20. Yu. S. Kivshar, W. Krolikowski: Opt. Commun. **114**, 353 (1995)
21. J.S. Aitchison, Y. Silberberg, A.M. Weiner, D.E. Leaird, M.K. Oliver, J.L. Jackel, E.M. Vogel, P.W.E. Smith: J. Opt. Soc. Am. B **8**, 1290 (1991)
22. B. Luther-Davies, R. Powles, V. Tikhonenko: Opt. Lett. **15**, 1816 (1994)
23. D.C. Hutchings, B.S. Wherett: Opt. Commun. **111**, 507 (1994)
24. H. Ma, A.-S.L. Gomes, Cid B. de Araujo: Opt. Commun. **87**, 19 (1992)
25. M. Karlsson, D. Anderson, M. Desaix, M. Lisak: Opt. Lett. **16**, 1373 (1991)
26. D.E. Pelinowsky, Y.A. Stepanyants, Yu. S. Kivshar: Phys. Rev. E **51**, 5016 (1995)